ACCOUNTS
of chemical research

Vibrational Spectroscopy of Electronic Processes in Emerging Photovoltaic Materials

KWANG S. JEONG, RYAN D. PENSACK, AND JOHN B. ASBURY*

Department of Chemistry, The Pennsylvania State University, University Park, Pennsylvania 16802, United States

RECEIVED ON OCTOBER 31, 2012

CONSPECTUS

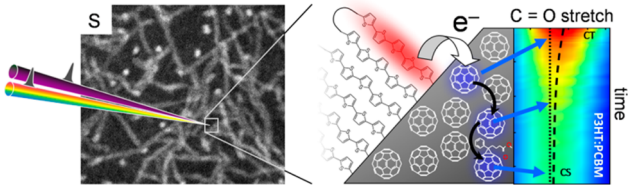

Molecules affect the electronic properties of many emerging materials, ranging from organic thin film transistors and light emitting diodes for flexible displays to colloidal quantum dots (CQDs) used in solution processed photovoltaics and photodetectors. For example, the interactions of conjugated molecules not only influence morphological and charge transport properties of organic photovoltaic (OPV) materials, but they also determine the primary photophysical events leading to charge generation. Ligand–nanocrystal interactions affect the density and energetic distributions of trap states, which in turn influence minority carrier transport in CQD photovoltaics. Therefore, it is critical for scientists to understand how the underlying molecular structures and morphologies determine the electronic properties of emerging materials.

Recently, chemists have used vibrational spectroscopy to study electronic processes in emerging materials, and been able to directly measure the influence molecular properties have on those processes. Time-resolved vibrational spectroscopy is uniquely positioned to examine molecular species involved in electronic processes because it combines ultrafast time resolution with measurement of the vibrational spectra of molecules. For instance, molecules at the electron donor/acceptor interfaces in OPV materials have unique vibrational features because vibrational frequencies of molecules are sensitive to their local molecular environments. Through ultrafast vibrational spectroscopy, researchers can directly examine the dynamics of charge transfer (CT) state formation and dissociation to form charge separated states specifically at donor/acceptor interfaces. Vibrational modes of ligands are also sensitive to their bonding interactions with nanocrystal surfaces, which enables chemists to directly probe the molecular nature of charge trap states in colloidal quantum dot solids. Because of the ability to connect electrical properties with the underlying molecular species, scientists can use ultrafast vibrational spectroscopy to address fundamental challenges in the development of emerging electronic materials.

In this Account, we focus on two applications of vibrational spectroscopy to examine electronic processes in OPV and CQD photovoltaic materials. In the first application, we examine archetypal classes of electron acceptors in OPV materials and reveal how their molecular structures influence the dynamics and energetic barriers to CT state formation and dissociation. In the second application, we discuss the surface chemistry of ligand–nanocrystal interactions and how they impact the density and energetic distribution of charge trap states in CQD photovoltaic materials. Through direct observations of the vibrational features of ligands attached to surface trap states, we can obtain valuable insights into the nature of charge traps and begin to understand pathways for their elimination. We expect that further examination of electronic processes in materials using ultrafast vibrational spectroscopy will lead to new design rules in support of continued materials development efforts.

1. Introduction

Many emerging electronic materials targeting high throughput low temperature processing are molecular in nature. Examples include organic semiconductors for organic thin film transistor, light emitting diode, and photovoltaic applications in which the active electronic materials consist of conjugated molecules[1,2] or polymers.[3,4] Inorganic material systems involving molecular moieties include colloidal quantum dot or nanocrystalline systems in which molecular ligands are used to passivate dangling bonds and control crystal growth.[5] Molecular ligands used in nanocrystalline systems are typically exchanged or removed to achieve

Published on the Web 03/20/2013 www.pubs.acs.org/accounts
10.1021/ar300300m

desirable material properties such as dense packing and high charge carrier mobility.

The utilization of molecular species either as active materials or as precursors causes the structure and characteristics of molecules to figure prominently in the electronic properties of many emerging materials.[6−8] Electrical techniques have long existed to characterize with high sensitivity charge carrier mobilities, defect state densities, and their energetic distributions in materials. However, the techniques do not provided detailed information about the molecular species that give rise to these properties. Ultraviolet, X-ray, and electron microscopy techniques commonly used to characterize materials are capable of providing chemically specific information. These techniques examine majority species in materials and as such have limited applicability to examine defects that are typically minority species.

Ultrafast infrared spectroscopy is uniquely positioned to examine molecular species in emerging electronic materials because it combines ultrafast time resolution with measurement of vibrational spectra of materials.[6−11] The method is not a replacement for traditional electrical characterization techniques but provides unique complementary information to draw closer the link between underlying molecular structure and the corresponding electronic properties. A summary of infrared spectroscopy techniques to examine fundamental charge separation, transport, and trapping processes in functional electronic materials has recently been reported.[12] This Account focuses on applications of the techniques to address (1) the influence of molecular structure on fundamental charge carrier dynamics in organic photovoltaic (OPV) materials[8,9] and (2) the surface chemistry of ligand−nanocrystal interactions and the influence that the associated trap states have on charge transport in colloidal quantum dot (CQD) photovoltaics.[6,7]

2. Charge Carrier Dynamics in OPVs

To date, fullerenes are unique in their ability to function as acceptors in high efficiency organic solar cells.[13] Considerable effort has focused on the development of alternatives to fullerenes as electron acceptors because the anticipated cost structure for manufacture of organic solar cells is more favorable if fullerenes can be replaced. Numerous promising alternative acceptors have been identified, but none have led to devices with power conversion efficiencies that approach those achievable with fullerene-based electron acceptors.[14]

In an effort to identify the origins of the apparent uniqueness of fullerenes as electron acceptors in organic solar cells,

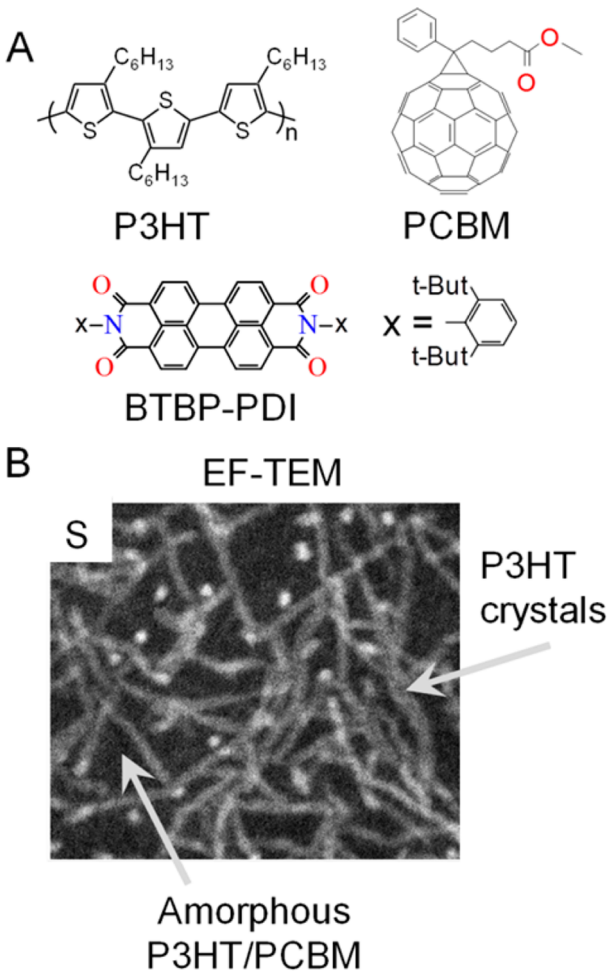

FIGURE 1. (A) Molecular structures of select organic semiconductors used to examine the influence that electron acceptor structure has on photocurrent generation in OPV materials. (B) Energy filtered transmission electron microscopy image representing a sulfur map of a 1:1 by mass P3HT:PCBM polymer blend. The polymer forms crystals imbedded in an amorphous mixture of the polymer and fullerene. (Adapted with permission from ref 8. Copyright 2012 American Chemical Society.)

solvatochromism assisted vibrational spectroscopy (SAVS)[15] was used to examine the primary events leading to charge separation in materials containing two archetypal classes of electron acceptors, fullerenes, and perylene diimides, blended with the conjugated polymer donor, regioregular poly(3-hexylthiophene) (P3HT, Figure 1A).[8] The fullerene derivative examined in the study, [6,6]-phenyl-C_{61}-butyric acid methyl ester (PCBM, Figure 1A), represents the class of pseudo-three-dimensional electron acceptors that have been successfully utilized in organic solar cells. In contrast, the perylene diimide derivative, bis-tertiarybutylphenyl substituted perylene diimide (BTBP-PDI, Figure 1A), represents pseudo-two-dimensional electron acceptors.

Understanding how electron acceptor structure influences the mechanisms of charge photogeneration in organic solar

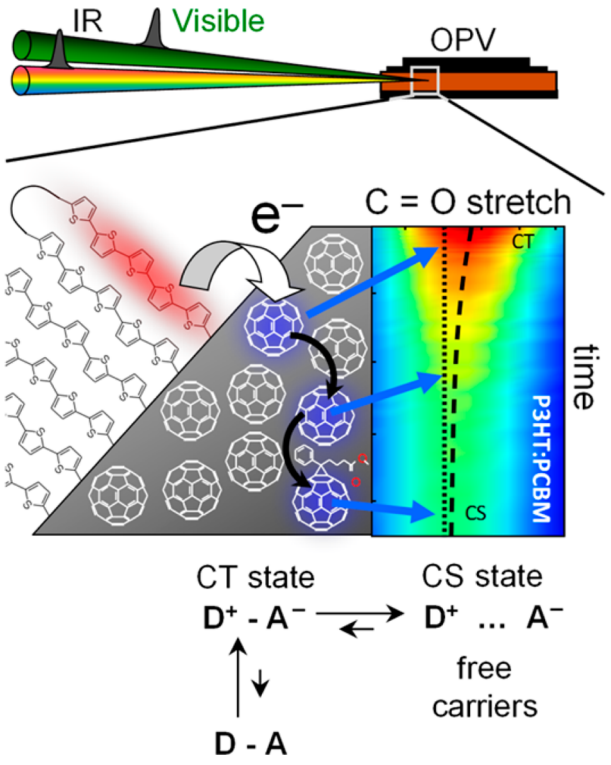

FIGURE 2. Illustration of the ultrafast SAVS approach to measure formation and dissociation dynamics of CT states specifically at interfaces in OPV materials. Following optical excitation, the dynamics of CT state dissociation are examined through the time-dependent evolution of the vibrational frequencies in the system. The SAVS approach enables unambiguous observation of charge transfer state (D^+-A^-) formation and subsequent dissociation to form charge separated states ($D^+\cdots A^-$). (Adapted from ref 15.)

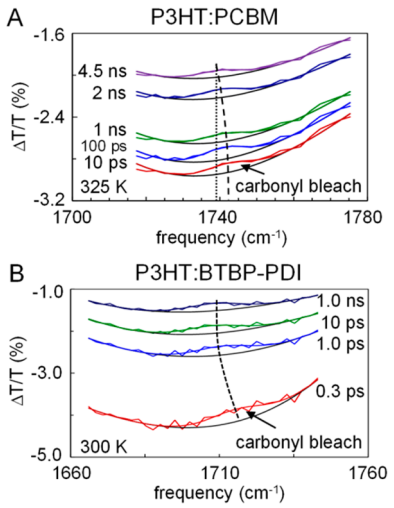

FIGURE 3. Transient visible pump-infrared probe spectra of (A) P3HT:PCBM polymer blend measured at 300 K and (B) P3HT:BTBP-PDI polymer blend measured at 325 K. Carbonyl bleach features due to electron transfer from photoexcited P3HT to the acceptors are superimposed on broad polaron absorptions. The time dependent shifts of the carbonyl bleach center frequencies to lower values are highlighted by the dashed curves. (Adapted with permission from ref 8. Copyright 2012 American Chemical Society.)

cells requires detailed investigation of electronic processes in materials such as that represented in the energy filtered transmission electron micrograph appearing in Figure 1B.[16,17] The image reveals an intricate network of electron/donor–acceptor interfaces where several processes occur that strongly influence the efficiency of photocurrent generation. The processes, represented in Figure 2, include light absorption to form excitons, electron transfer at donor/acceptor interfaces to form charge transfer (CT) states, and dissociation of CT states to form charge separated (CS) states.[18,19]

The SAVS approach takes advantage of the sensitivity of vibrational modes to their local molecular environments[20] to directly examine charge carrier dynamics specifically at interfaces. This sensitivity causes molecules at electron donor/acceptor interfaces that are involved in the formation of CT states to be distinguishable from molecules involved in CS states through differences in their vibrational frequencies. The cartoon in Figure 2 depicts this sensitivity and its use to directly examine charge separation. Because CT states initially form at donor–acceptor interfaces,[18] electrons occupy acceptor molecules having unique vibrational frequencies due to solvatochromism. As electrons dissociate from CT states to form CS states, they occupy molecules having lower vibrational frequencies. This process gives rise to transient vibrational features exhibiting time-dependent frequency shifts that can be monitored to directly measure the time scales for CT state dissociation.[9]

The ultrafast SAVS approach consists of several ultrafast vibrational spectroscopy techniques used in concert. Two-dimensional infrared[21] and other infrared pump–probe techniques[9] are used to characterize the dynamics of vibrational modes of molecules in their ground electronic state potentials. Photophysical and photochemical processes are examined through the frequency evolution of vibrational modes using ultrafast visible pump-infrared probe experiments.[9] To date, the SAVS approach has been applied to electron acceptors with carbonyl vibrations. Molecules with other vibrational modes can now be examined opening opportunities to study a wide array of organic semiconductor systems.

Ultrafast infrared transient absorption spectra measured around 300 K at several time delays following visible excitation of polymer blends incorporating PCBM and BTBP-PDI appear in Figure 3A and B, respectively.[8] The conjugated polymer, P3HT, serves as the electron donor in both systems. The spectra exhibit broad electronic transitions characteristic

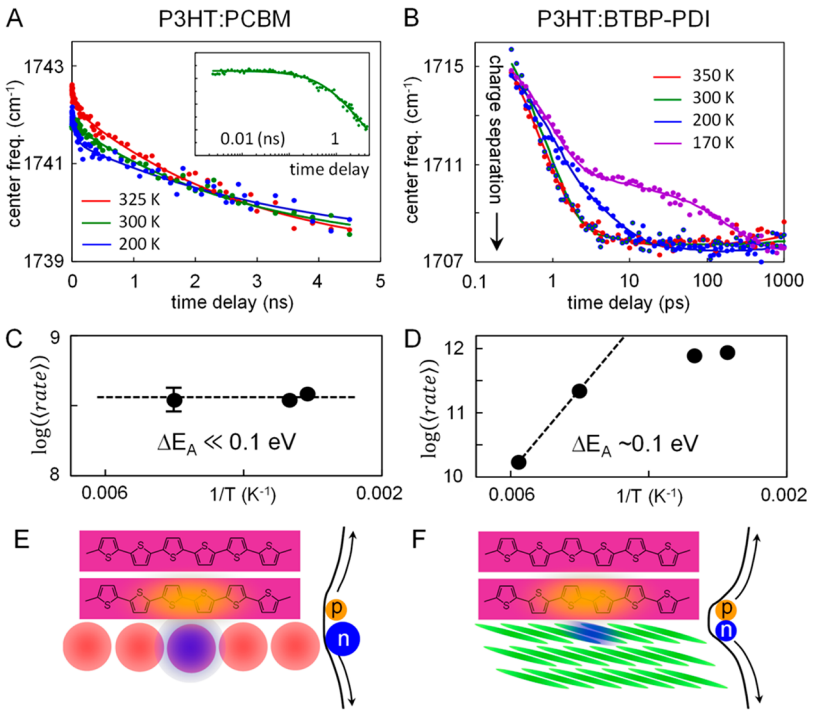

FIGURE 4. Time dependent carbonyl bleach center frequencies obtained from P3HT:PCBM (A) and P3HT:BTBP-PDI (B) polymer blends versus the corresponding time delays for several temperatures. The inset in panel A demonstrates that charge separation occurs on the nanosecond time scale in the P3HT:PCBM blend. Plots of the logarithms of the average rates of charge separation versus inverse temperature in the P3HT:PCBM and P3HT:BTBP-PDI are displayed in panels C and D, respectively. Schematic diagrams of the influence of molecular structure on the delocalization of electronic wave functions and free energy barriers to charge separation are displayed in panels E and F for the PCBM and PDI blends with P3HT. The data suggest that PDI molecules with two-dimensional topology exhibit stronger Coulomb forces and larger reorganization energies to charge separation in comparison to fullerenes that have three-dimensional topology. (Adapted from ref 12.)

of polaron absorptions in conjugated polymers that are superimposed onto transient vibrational features of the carbonyl stretch modes of the acceptors. The transient vibrational spectra, termed carbonyl bleach features, arise from the depletion of neutral ground state acceptor molecules due to electron transfer from P3HT. The dashed curves in both sets of transient absorption spectra highlight the time evolution of the center frequencies of the carbonyl bleach features. The shift of the carbonyl bleach spectra toward the equilibrium center frequencies has been shown to result from CT state dissociation at electron donor/acceptor interfaces to form CS states.[9,15]

2.1. Influence of Acceptor Structure on Barriers to Charge Separation. The influence that acceptor structure has on free energy barriers to charge separation in OPV materials can be examined by temperature dependent measurements of the charge separation process using SAVS.[8] Figure 4A and B displays the time-dependent center frequencies of the carbonyl stretch modes of PCBM and BTBP-PDI in their respective blends with P3HT plotted versus the corresponding time delays at which the transient spectra were measured. In both cases, the time dependent frequency shifts are indicative of the time scale for charge separation. Approximate barriers to charge separation are obtained from analysis of the temperature-dependence of charge separation rates in both systems. Figure 4C and D represents the logarithms of the average rates plotted versus inverse temperature for the PCBM and BTBP-PDI blends with P3HT, respectively. The logarithms of the average rates of charge separation in the P3HT:PCBM blend appearing in Figure 4C are temperature invariant within experimental precision indicated by the error bar. The data demonstrate that charge separation occurs by an activationless pathway in accord with temperature dependent measurements of charge photogeneration in P3HT:PCBM photovoltaic devices.[22,23]

In contrast to the weak temperature dependence observed in the PCBM polymer blend, the rate of charge separation in the blend of P3HT with BTBP-PDI depends sensitively on temperature, indicating that the process occurs via a thermally activated pathway.[8] An approximate activation energy of 0.1 eV is obtained by consideration of the slope of the line formed by the lowest temperature data points. This value for the activation energy should only be considered approximate given the limited data set from

which it is obtained. The transition from stronger to weaker temperature dependence between 200 and 300 K occurs when the time scale of charge separation approaches the free-induction decay time of the carbonyl vibrational modes. Frequency shift dynamics occurring faster than the free-induction decay time affect the spectrum of the vibrational mode rather than the time-dependence of the center frequency. The SAVS approach is currently being extended to examine other vibrational modes with broader spectral linewidths that will enable exploration of faster charge separation.

The observation of distinct barriers to charge separation in the P3HT:PCBM versus P3HT:BTBP-PDI polymer blends can be understood in terms of the influence of molecular topology on delocalization of electronic wave functions as represented in Figure 4E and F. Prior temperature dependent measurements of electron transfer rates demonstrate that increased delocalization leads to weak temperature dependence[24,25] because of the smaller associated reorganization energies.[25,26] Increased delocalization also gives rise to more distributed charge distributions within CT states such that the Coulomb binding energy of electron hole pairs is smaller. Applied specifically to the PCBM system, electrons transferred to PCBM molecules are capable of delocalizing over the entire conjugated framework of the fullerene. Because fullerenes are comparatively large (each is about 1 nm^3), electron delocalization onto only a few molecules enables extended charge densities that are close to the Coulomb capture radius of ~10 nm when energetic disorder is taken into account.[18]

In contrast, the conjugated framework of BTBP-PDI molecules is smaller, planar, and anisotropic. As represented in Figure 4F, the smaller, planar structure requires that electron density be delocalized over many more PDI molecules to obtain similar delocalization of charge distributions as can be achieved with fullerenes. X-ray diffraction studies indicate that BTBP-PDI molecules are not highly crystalline in blends with P3HT[8] but are more crystalline than PCBM.[27] Although the electronic coupling between PDI molecules can on average be greater than between fullerenes (as seen in the faster charge separation dynamics in BTBP-PDI system), the coupling strength between anisotropic molecules depends sensitively on both intermolecular distances and angles.[28] Consequently, planar conjugated molecules are less able to accommodate disorder while still supporting charge delocalization and efficient charge transport.

2.2. Influence of Acceptor Structure on Photovoltaic Devices. The observation of distinctly different energetic barriers to charge separation in the P3HT:PCBM versus the P3HT:BTBP-PDI polymer blends suggests that Coulomb forces are stronger and reorganization energies are larger in the BTBP-PDI system. A key prediction based on this conclusion is that charge recombination (geminate and bimolecular) should be more pronounced in the P3HT:BTBP-PDI polymer blend than in the P3HT:PCBM blend. The light and dark current–voltage (I–V) curves (Figure 5) measured in optimized organic solar cells fabricated using the P3HT:PCBM (upper panel) and P3HT:BTBP-PDI (lower panel) polymer blends are consistent with this prediction. The data reveal a 20-fold reduction in photocurrent in the P3HT:BTBP-PDI device. It is understood that the photocurrent collected from a solar cell is determined by a number of factors including light absorption, exciton splitting, CT state dissociation, and charge transport. However, the observation of 20-fold reduction in photocurrent provides confirmation that indeed charge generation and transport are significantly reduced in the P3HT:BTBP-PDI polymer blend.

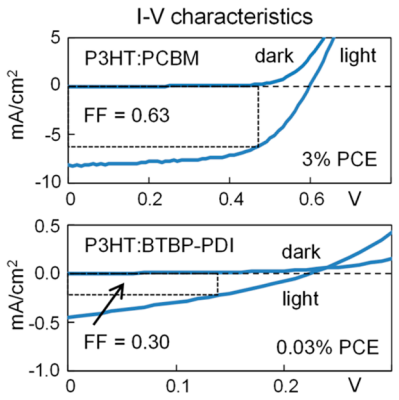

FIGURE 5. Comparison of I–V curves of photovoltaic devices measured under 100 mA/cm^2 simulated solar illumination (curves labeled light) and under dark (curves labeled dark) conditions. The upper and lower panels represent data measured in devices containing P3HT:PCBM and P3HT:BTBP-PDI polymer blend active layers, respectively.

The shapes of the I–V curves in Figure 5 can be further interpreted using a model proposed by Giebink and coworkers[29,30] who showed that electrical properties of OPV devices such as open-circuit voltage (V_{OC}) and fill factor (FF) are strongly influenced by electron donor/acceptor electronic coupling and by competition between CT state dissociation and recombination (termed polaron pair recombination[29,30]). Indeed, improvements of the V_{OC} and FF of organic solar cells have been correlated with lower electronic coupling and greater energetic disorder specifically at donor/acceptor interfaces.[31,32] Viewing the I–V curves in Figure 5 from this perspective, the lower V_{OC} of the P3HT:BTBP-PDI devices suggest stronger donor/acceptor

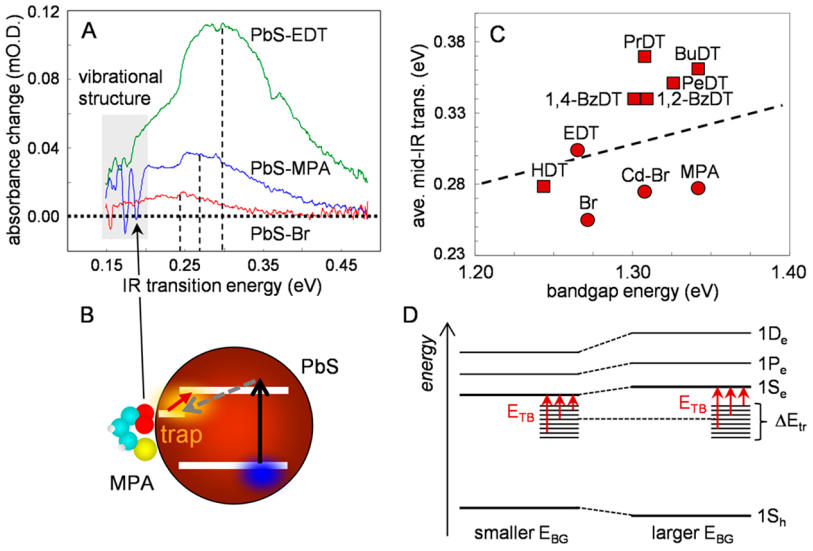

FIGURE 6. (A) Time-resolved infrared spectra of PbS CQD films passivated by EDT, MPA, and Br^- measured 500 ns following optical excitation of the bandgap of the films. Narrow vibrational features are superimposed onto broad electronic transitions. (B) Cartoon illustrating the origin of trap-to-band transitions giving rise to the broad electronic transitions observed in the spectra. (C) Comparison of the band gap transition energies with the corresponding average mid-IR transition energies of PbS CQD films treated with various ligands. (D) Schematic diagram illustrating the origin of trap-to-band transitions in quantum dots. The large ligand-related scatter coupled with the appearance of ligand vibrational features indicate that trap-to-band transitions are responsible for the broad electronic transitions appearing in panel A. (Adapted from refs 6 and 7 (Copyright 2012 American Chemical Society)).

electronic coupling and less efficient CT dissociation in comparison to the PCBM system (from consideration of their excited state energy levels). The SAVS studies provide independent support for this interpretation. The faster CT state dissociation observed in the P3HT:BTBP-PDI polymer blend indicates that BTBP-PDI molecules are more strongly coupled to each other and by extension to neighboring P3HT conjugated segments. The observation of activated charge separation in the P3HT:BTBP-PDI system and interpretation in terms of more localized charge distributions is consistent with stronger Coulomb forces that bind hole/electron pairs to donor/acceptor interfaces, leading to lower net efficiency of CT state dissociation. Because device performance can depend on many variables that are not always controlled, it is generally difficult to interpret the shapes of *I*–*V* curves in terms of specific molecular interactions. This example highlights the type of complementary information obtained from SAVS studies that enables detailed interpretation of *I*–*V* curves in terms of specific influences that acceptor molecular structures have on the electrical properties of OPV materials.

3. Charge Trapping in Colloidal Quantum Dot Photovoltaics

Colloidal quantum dot or nanocrystal materials combine favorable properties of near-IR absorption, delocalized wave functions, and high dielectric permittivity of inorganic semiconductors with the solution processability and flexibility of organic or hybrid materials.[33] The need to maximize electronic overlap of nanocrystals while simultaneously minimizing the density of surface defect states for efficient charge transport creates new opportunities to understand and control the interaction of ligands with nanocrystal surfaces.[34] A number of strategies have been explored in an effort to achieve this balance in metal chalcogenide CQD materials.[6,35–38] These efforts have yielded dramatic gains in majority carrier field effect mobilities in CQD films.[37] However, minority carrier mobilities, that strongly affect photovoltaic device performance, indicate further improvements are needed in surface passivation for continued development of CQD materials as high efficiency photovoltaics.[33,35,36] Because it can be challenging to characterize the extent of ligand exchange in nanocrystalline materials,[39] new experimental methods are needed to correlate the density and energetic distribution of surface defect states with the underlying ligand-nanocrystal interactions that give rise to those states.[6,7]

TRIR spectroscopy was recently combined with electrical measurements to examine charge recombination lifetimes and carrier mobilities of PbS CQD photovoltaic materials and to correlate those properties with the underlying ligand-nanocrystal interactions.[6,7] The transient infrared spectra appearing in Figure 6A were measured at 500 ns time delay following 532 nm excitation of PbS CQD films treated with

1,2-ethanedithiol (PbS-EDT), 3-mercaptopropionic acid (PbS-MPA), and bromide ions (PbS-Br). In all cases, the PbS films were deposited under conditions identical to state of the art photovoltaic devices used for the electrical measurements.

Two principal spectroscopic features appear in each spectrum: broad electronic transitions covering the mid-infrared (mid-IR) region and narrow vibrational features corresponding to functional groups of the ligands. The sequence of light−matter interactions giving rise to these features is summarized schematically in Figure 6B. First, excitons are created by bandgap excitation of the PbS CQDs resulting in electrons and holes in delocalized states of the nanocrystals. Excitons can relax radiatively or nonradiatively back to the ground electronic state or dissociate via interdot electron transfer to form free carriers that move through the film or become trapped. The latter trapping process is depicted in Figure 6B as the dashed diagonal arrow (subsequent recombination or re-emission to band states are not shown). The broad electronic transitions appearing in Figure 6A arise from mid-IR excitation of trapped carriers (electrons in the case of p-doped films) back into core states of the nanocrystals. These transitions, termed trap-to-band transitions,[6] are depicted as the solid diagonal arrow in Figure 6B.

3.1. Assignment of Trap-to-Band Transitions. Assignment of the broad mid-IR electronic transitions appearing in Figure 6A to trap-to-band transitions rather than intraband transitions is based on lack of correlation of the mid-IR transition energies with the bandgaps of the PbS CQDs and on the appearance of transient vibrational features of the ligands.[7] Figure 6C represents a collection of average mid-IR transition energies measured in PbS CQD films treated with a variety of small ligands plotted versus the corresponding bandgap transition energies of the films. The data labels correspond to the acronyms for the ligands used to treat the films: EDT = 1,2-ethanedithiol; PrDT = 1,3-propanedithiol; BuDT = 1,4-butanedithiol; PeDT = 1,5-pentanedithiol; HDT = 1,6-hexanedithiol; 1,2-BzDT = 1,2-benzenedithiol; 1,4-BzDT = 1,4-benzenedithiol; MPA = 3-mercaptopropionic acid; Br− bromide; and Cd−Br = bromide treated films pretreated with Cd-tetradecylphosphonic acid. The data reveal little or no correlation that would be expected between the mid-IR and bandgap transitions if the mid-IR transitions arose from intraband transitions such as those observed in colloidal solutions of CdSe quantum dots.[40,41]

Instead, the variation of mid-IR transition energies of the PbS films is dominated by the nature of the ligands used to passivate the PbS surfaces possibly via mixing of surface and core states.[42] Consequently, the broad electronic transitions appearing in Figure 6A are assigned to trap-to-band transitions in which electrons (holes) are excited from localized states associated with the ligands back into delocalized core states of the quantum dots.[7] The vertical arrows connecting the below-gap states labeled ΔE_{tr} in Figure 6D represent schematically the trap-to-band transitions observed in the PbS CQD films.

The appearance of narrow vibrational features in Figure 6A provides further support of the trap-to-band transition assignment. Excitation of electrons or holes from localized surface trap states to core states of the CQDs changes the charge distributions experienced by the surface bound functional groups of the ligands. The effect is most pronounced in the MPA treated PbS films because the carboxylate group is a strong infrared chromophore and is directly attached to the quantum dot surfaces. The narrow negative-going vibrational features in the PbS-MPA spectrum around 0.18 eV (1405 and 1520 cm^{-1}) correspond to the vibrational spectra of carboxylate groups attached to Pb sites[43] before electrons (holes) are localized in the vicinity of the ligands. After localization, the spectra of the carboxylate groups shift to lower frequency giving rise to the positive-going peaks on the lower frequency side of the negative-going features. PbS CQD films treated with other ligands exhibit similar perturbations specific to their vibrational spectra due to the localization of charge carriers near their surfaces.

Importantly, the initial amplitude of the trap-to-band transitions appearing in Figure 6A are correlated with the measured band-tail density of states below the conduction band in PbS CQD films treated with EDT,[35] MPA,[36] and Br^{-}[6] ligands. The band-tail density of states in the films, obtained from zero-bias capacitance measurements, reveal a 20-fold reduction in the trap state density comparing EDT and Br^{-} passivated PbS CQD films. The trap-to-band transition intensities exhibit a 10-fold reduction comparing the same films, further supporting the assignment of the transitions to the absorption of trap carriers in the nanocrystalline materials.

3.2. Ligand−Nanocrystal Interactions Influence Electrical Properties. The ability to probe trap-to-band transitions in PbS CQDs provides opportunities to understand how ligand-nanocrystal interactions affect the electrical properties of the corresponding photovoltaic materials. For example, the time-dependent amplitudes of trap-to-band transitions can be used as a direct measure of charge recombination

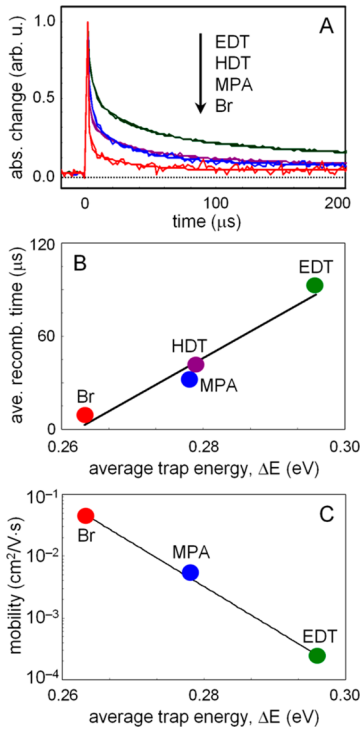

FIGURE 7. (A) Kinetics traces measured at the peaks of trap-to-band transitions of PbS CQD films following optical excitation indicating the dynamics of charge recombination. (B) Plot of the average charge recombination lifetimes versus the average trap energies measured from transient infrared spectra of the corresponding films. (C) Plot of the minority carrier (electron) mobility of PbS CQD films versus the average charge trap energy of the films. The reduced charge trap density of the Br^- passivated film results in a 20-fold increase in the mobility-lifetime product in comparison to the EDT treated film. (Adapted from ref 6.)

dynamics.[7] Kinetic decay traces appearing in Figure 7A represent the dynamics of charge recombination in EDT, HDT, MPA, and Br^- treated PbS CQD films following bandgap excitation of the films. The average charge recombination lifetimes of films are displayed in Figure 7B versus the corresponding average trap energy. The data reveal that the average charge recombination lifetime is correlated with the average charge trap depth in PbS nanocrystals. Importantly, there is a 10-fold reduction of the charge recombination lifetime comparing the Br^- and EDT treated films.

Thin film transistor measurements of PbS CQD films passivated by EDT, MPA, and Br^- demonstrate that the minority carrier mobility increases 200-fold comparing EDT and Br^- treated films (Figure 7C).[6] The variations among the charge recombination lifetimes and charge carrier mobilities are anticorrelated as expected for diffusion controlled bimolecular charge recombination processes. However, the increase in electron mobility is much greater than the

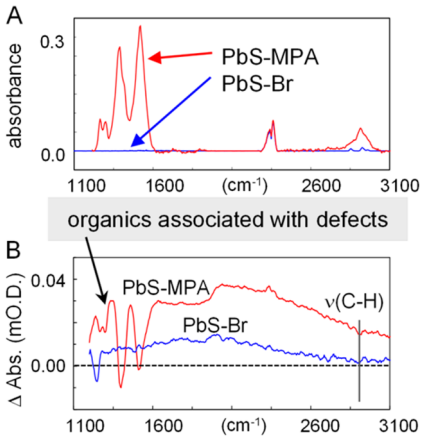

FIGURE 8. (A) Infrared absorption spectra PbS CQD films passivated by MPA and Br^- ligands. (B) Transient infrared absorption spectra of the corresponding PbS CQD films measured 500 ns following bandgap excitation. The Br^- treated film exhibits a vibrational feature around 1300 cm^{-1} indicating that residual organic species closely associated with charge traps remain in the film.

corresponding decrease in charge recombination lifetime of the Br^- passivated PbS CQD films. These findings indicate that ligand–nanocrystal interactions, tuned by the choice of passivating ligands and material processing conditions, strongly impact the mobility-lifetime products of CQD materials.[7] The improvements in charge trap density and electron mobility comparing EDT, MPA, and Br^- passivated films are associated with significant gains in power conversion efficiency ranging from 2% for EDT treated devices[35] to 6% for Br^- treated devices.[6]

Time-resolved infrared spectroscopy is uniquely positioned to identify molecular species in materials that are associated with defects through their vibrational modes. An example highlighting this capability is represented in Figure 8. The infrared absorption spectra appearing in Figure 8A were measured in MPA and Br^- treated PbS CQD films. The spectrum of the MPA treated film exhibits vibrational features that are characteristic of the organic ligand. The absence of vibrational features in the spectrum of the Br^- treated film results from ligand exchange chemistry that is designed to replace all organic ligands with the Br^- ions[6] such that all vibrational modes of the material are expected to be low frequency. Represented in Figure 8B are time-resolved infrared spectra of the MPA and Br^- treated PbS CQD films measured 500 ns after 532 nm excitation. The transient spectra of both films exhibit broad trap-to-band transitions with superimposed narrow vibrational features. In the case of the MPA treated film, the appearance of the vibrational features is expected and indicates the perturbation of carboxylic vibrational modes of the ligands by charge

trapping. Surprisingly, narrow vibrational features are also observed in the Br^- treated film even though no organic species are supposed to be present in the film. The appearance of this feature indicates that residual organic species remain in the film and that they are closely associated with charge traps. These findings suggest that more complete removal of residual organic species will decrease the density of charge traps with corresponding improvements in electron mobility, CQD film density, and device power conversion efficiency.

4. Conclusions and Future Directions

The emergence of materials targeting solution phase or low temperature processing is creating new opportunities to understand the influences that molecular structure and composition have on electronic properties of materials. The example material systems described here highlight some of the capabilities that come with the use of infrared spectroscopy to probe the nature and dynamics of transient electronic species through their vibrational features. For OPVs, the sensitivity of vibrational modes to their local molecular environments provides opportunities to probe electronic processes specifically at electron donor/acceptor interfaces and to elucidate the influence that molecular structure and crystallinity have on the primary events leading to photocurrent generation. In colloidal quantum dot photovoltaics, vibrational modes of ligands are sensitive to ligand–nanocrystal interactions and local electrostatic potentials. Probing the vibrations of ligands provides a means to correlate the density and energetic distribution of charge traps to the underlying ligand–nanocrystal interactions. It is expected that the examples included in this Account will motivate continued development of vibrational spectroscopy techniques to understand and ultimately control the influences that molecular structures have on electronic processes in emerging materials.

The work discussed in this Account results from the efforts of many exceptional people with whom the authors have been privileged to work. Special thanks go to Prof. Enrique D. Gomez, Changhe Guo, and Kiarash Vakhshouri from the Pennsylvania State University for electrical measurements and energy filtered transmission electron microscopy images of OPV materials and devices. The authors also thank Prof. Edward H. Sargent, Dr. Jiang Tang, and Kyle Kemp at the University of Toronto for supplying PbS CQDs, film deposition procedures, and electrical characterization of PbS CQD films. This research was supported by the National Science Foundation (CHE-0846241 and DMR-0820404), the Office of Naval Research (N00014-11-1-0239), and the Petroleum Research Fund (49639-ND6).

BIOGRAPHICAL INFORMATION

Kwang S. Jeong earned a B.S. from Korea University (2007) and is a Ph.D. candidate at the Pennsylvania State University. His research focuses on the use of ultrafast vibrational spectroscopy to examine ligand–nanocrystal interactions giving rise to charge traps in colloidal quantum dot photovoltaic materials.

Ryan D. Pensack earned a B.S. from Rutgers University (2006) and a Ph.D. from the Pennsylvania State University (2012) using ultrafast vibrational spectroscopy to examine mechanisms of charge separation in OPV materials. He began a postdoctoral fellowship at the University of Toronto in 2012.

John B. Asbury earned a B.S. from the University of Tennessee (1996), a Ph.D. at Emory University (2001) and did postdoctoral work at Stanford University until 2005. Since 2005, he has been a professor of chemistry at the Pennsylvania State University with a research focus on the development of ultrafast vibrational spectroscopy techniques to examine the influences of molecular structure on fundamental charge carrier dynamics in emerging electronic materials.

FOOTNOTES

*To whom correspondence should be addressed.
The authors declare no competing financial interest.

REFERENCES

1 Forrest, S. R. Path to Ubiquitous and Low-cost Organic Electronic Appliances on Plastic. *Nature* **2004**, *428*, 911–918.
2 Anthony, J. E. Functionalized Acenes and Heteroacenes for Organic Electronics. *Chem. Rev.* **2006**, *106*, 5028–5048.
3 Gunes, S.; Neugebauer, H.; Sariciftci, N. S. Conjugated Polymer-Based Organic Solar Cells. *Chem. Rev.* **2007**, *107*, 1324–1338.
4 Li, G.; Zhu, R.; Yang, Y. Polymer Solar Cells. *Nat. Photonics* **2012**, *6*, 153–161.
5 Murray, C. B.; Kagan, C. R.; Bawendi, M. G. Synthesis and Characterization of Monodisperse Nanocrystals and Close-packed Nanocrystal Assemblies. *Annu. Rev. Mater. Sci.* **2000**, *30*, 545–610.
6 Tang, J.; Kemp, K.; Hoogland, S.; Jeong, K. S.; Liu, H.; Levina, L.; Furukawa, M.; Wang, X.; Debnath, R.; Cha, D.; Chou, K. W.; Fischer, A.; Amassian, A.; Asbury, J. B.; Sargent, E. H. Colloidal Quantum Dot Photovoltaics Using Atomic Ligand Passivation. *Nat. Mater.* **2011**, *10*, 765–771.
7 Jeong, K. S.; Tang, J.; Liu, H.; Kim, J.; Schaefer, A. W.; Kemp, K.; Levina, L.; Wang, X.; Hoogland, S.; Debnath, R.; Brzozowski, L.; Sargent, E. H.; Asbury, J. B. Enhanced Mobility-Lifetime Products in Colloidal Quantum Dot Photovoltaics. *ACS Nano* **2012**, *6*, 89–99.
8 Pensack, R. D.; Guo, C.; Vakhshouri, K.; Gomez, E. D.; Asbury, J. B. Influence of Acceptor Structure on Barriers to Charge Separation in Organic Photovoltaic Materials. *J. Phys. Chem. C* **2012**, *116*, 4824–4831.
9 Barbour, L. W.; Hegadorn, M.; Asbury, J. B. Watching Electrons Move in Real Time: Ultrafast Infrared Spectroscopy of a Polymer Blend Photovoltaic Material. *J. Am. Chem. Soc.* **2007**, *129*, 15884–15894.
10 Anglin, T. C.; Sohrabpour, Z.; Massari, A. M. Nonlinear Spectroscopic Markers of Structural Change During Charge Accumulation in Organic Field-Effect Transistors. *J. Phys. Chem. C* **2011**, *115*, 20258–20266.
11 O'Brien, D. B.; Anglin, T. C.; Massari, A. M. Surface Chemistry and Annealing-Driven Interfacial Changes in Organic Semiconducting Thin Films on Silica Surfaces. *Langmuir* **2011**, *27*, 13940–13949.
12 Asbury, J. B. Ultrafast Infrared Probes of Electronic Processes in Materials. In *Ultrafast Infrared Vibrational Spectroscopy*; Fayer, M. D., Ed.; Taylor and Francis: Boca Raton, FL, 2013; pp 239–267.
13 Peet, J.; Heeger, A. J.; Bazan, G. "Plastic" Solar Cells: Self-Assembly of Bulk Heterojunction Nanomaterials by Spontaneous Phase Separation. *Acc. Chem. Res.* **2009**, *42*, 1700–1708.

14 Anthony, J. E. Small-Molecule, Nonfullerene Acceptors for Polymer Bulk Heterojunction Organic Photovoltaics. *Chem. Mater.* **2011**, *23*, 583–590.

15 Pensack, R. D.; Asbury, J. B. Ultrafast Probes of Charge Transfer States in Organic Photovoltaic Materials. *Chem. Phys. Lett.* **2011**, *515*, 197–205.

16 Vakhshouri, K.; Kozub, D. R.; Wang, C.; Salleo, A.; Gomez, E. D. Effect of Miscibility and Percolation on Electron Transport in Amorphous Poly(3-Hexylthiophene)/Phenyl-C61-Butyric Acid Methyl Ester Blends. *Phys. Rev. Lett.* **2012**, *108*, 026601(5).

17 Kozub, D. R.; Vakhshouri, K.; Orme, L. M.; Wang, C.; Hexemer, A.; Gomez, E. D. Polymer Crystallization of Partially Miscible Polythiophene/Fullerene Mixtures Controls Morphology. *Macromolecules* **2011**, *44*, 5722–5726.

18 Clarke, T. M.; Durrant, J. R. Charge Photogeneration in Organic Solar Cells. *Chem. Rev.* **2010**, *110*, 6736–6767.

19 Bredas, J.-L.; Norton, J. E.; Cornil, J.; Coropceanu, V. Molecular Understanding of Organic Solar Cells: The Challenges. *Acc. Chem. Res.* **2009**, *42*, 1691–1699.

20 Pensack, R. D.; Banyas, K. M.; Asbury, J. B. Vibrational Solvatochromism in Organic Photovoltaic Materials: Method to Distinguish Molecules at Donor/Acceptor Interfaces. *Phys. Chem. Chem. Phys.* **2010**, *12*, 14144–14152.

21 Pensack, R. D.; Banyas, K. M.; Asbury, J. B. Temperature Independent Vibrational Dynamics in an Organic Photovoltaic Material. *J. Phys. Chem. B* **2010**, *114*, 12242–12251.

22 Iee, J.; Vandewal, K.; Yost, S. R.; Bahlke, M. E.; Goris, L.; Baldo, M. A.; Manca, J. V.; Van Voorhis, T. Charge Transfer State Versus Hot Exciton Dissociation in Polymer-Fullerene Blended Solar Cells. *J. Am. Chem. Soc.* **2010**, *132*, 11878–11880.

23 Grzegorczyk, W. J.; Savenije, T. J.; Dykstra, T. E.; Piris, J.; Schins, J. M.; Siebbeles, L. D. A. Temperature-Independent Charge Carrier Photogeneration in P3HT-PCBM Blends with Different Morphology. *J. Phys. Chem. C* **2010**, *114*, 5182–5186.

24 Trosken, B.; Willig, F.; Schwarzburg, K.; Ehret, A.; Spitler, M. The Primary Steps in Photography: Excited J-Aggregates on AgBr Microcystals. *Adv. Mater.* **1995**, *7*, 448–450.

25 Trosken, B.; Willig, F.; Schwarzburg, K.; Ehert, A.; Spitler, M. Electron Transfer Quenching of Excited J-Aggregate Dyes on AgBr Microcrystals Between 300 and 5 K. *J. Phys. Chem.* **1995**, *99*, 5152–5160.

26 Siebrand, W.; Ries, B.; Bassler, H. Theoretical Investigation of Optical Charge Carrier Generation Processes in Anthracene Crystals. *J. Mol. Electron.* **1987**, *337*, 218–227.

27 Gomez, E. D.; Barteau, K. P.; Wang, H.; Toney, M. F.; Loo, Y.-L. Correlating the Scattered Intensities of P3HT and PCBM to the Current Densities of Polymer Solar Cells. *Chem. Commun.* **2011**, *47*, 436–438.

28 Rand, B. P.; Cheyns, D.; Vasseur, K.; Giebink, N. C.; Mothy, S.; Yi, Y. P.; Coropceanu, V.; Beljonne, D.; Cornil, J.; Bredas, J.-L.; Genoe, J. The Impact of Molecular Orientation on the Photovoltaic Properties of a Phthalocyanine/Fullerene Heterojunction. *Adv. Funct. Mater.* **2012**, *22*, 2987–2995.

29 Giebink, N. C.; Wiederrecht, G. P.; Wasielewski, M. R.; Forrest, S. R. Ideal Diode Equation for Organic Heterojunctions. I. Derivation and Application. *Phys. Rev. B* **2010**, *82*, 155305(12).

30 Giebink, N. C.; Lassiter, B. E.; Wiederrecht, G. P.; Wasielewski, M. R.; Forrest, S. R. Ideal Diode Equation for Organic Heterojunctions. II. The Role of Polaron Pair Recombination. *Phys. Rev. B* **2010**, *82*, 155306(8).

31 Zimmermann, J. D.; Xiao, X.; Renshaw, K.; Wang, S.; Diev, V. V.; Thompson, M. E.; Forrest, S. R. Independent Control of Bulk and Interfacial Morphologies of Small Molecular Weight Organic Heterojunction Solar Cells. *Nano Lett.* **2012**, *12*, 4366–4371.

32 Erwin, P.; Thompson, M. E. Elucidating the Interplay Between Dark Current Coupling and Open Circuit Voltage in Organic Photovoltaics. *Appl. Phys. Lett.* **2011**, *98*, 223305(3).

33 Tang, J.; Sargent, E. H. Infrared Colloidal Quantum Dots for Photovoltaics: Fundamentals and Recent Progress. *Adv. Mater.* **2011**, *23*, 12–29.

34 Gratzel, M.; Janssen, R. A. J.; Mitzi, D. B.; Sargent, E. H. Materials Interface Engineering for Solution-Processed Photovoltaics. *Nature* **2012**, *488*, 304–312.

35 Tang, J.; Brzozowski, L.; Barkhouse, D. A. R.; Wang, X.; Debnath, R.; Wolowiec, R.; Palmiano, E.; Levina, L.; Pattantyus-Abraham, A. G.; Jamakosmanovic, D.; Sargent, E. H. Quantum Dot Photovoltaics in the Extreme Quantum Confinement Regime: The Surface-Chemical Origins of Exceptional Air- and Light-Stability. *ACS Nano* **2010**, *4*, 869–878.

36 Pattantyus-Abraham, A. G.; Kramer, I. J.; Barkhouse, A. R.; Wang, X.; Konstantatos, G.; Debnath, R.; Levina, L.; Nazeeruddin, M. K.; Gratzel, M.; Sargent, E. H. Depleted-Heterojunction Colloidal Quantum Dot Solar Cells. *ACS Nano* **2010**, *4*, 3374–3380.

37 Chung, D. S.; Lee, J. S.; Huang, J.; Nag, A.; Ithurria, S.; Talapin, D. V. Low Voltage, Hysteresis Free, and High Mobility Transistors from All-Inorganic Colloidal Nanocrystals. *Nano Lett.* **2012**, *12*, 1813–1820.

38 Talapin, D. V.; Murray, C. B. PbSe Nanocrystal Solids for n- and p-Channel Thin Film Field-Effect Transistors. *Science* **2005**, *310*, 86–89.

39 Owen, J. S.; Park, J.; Trudeau, P.-E.; Alivisatos, A. P. Reaction Chemistry and Ligand Exchange at Cadmium-Selenide Nanocrystal Surfaces. *J. Am. Chem. Soc.* **2008**, *130*, 12279–12281.

40 Shim, M.; Shilov, S. V.; Braiman, M. S.; Guyot-Sionnest, P. Long-Lived Delocalized Electron States in Quantum Dots: A Step-Scan Fourier Transform Infrared Study. *J. Phys. Chem. B* **2000**, *104*, 1494–1496.

41 Pandey, A.; Guyot-Sionnest, P. Intraband Spectroscopy and Band Offsets of Colloidal II-VI Core/Shell Structures. *J. Chem. Phys.* **2007**, *127*, 104710(10).

42 Wolcott, A.; Doyeux, V.; Nelson, C. A.; Gearba, R.; Lei, K.-W.; Yager, K. G.; Dolocan, A. D.; Williams, K.; Nguyen, D.; Zhu, X.-Y. Anomalously Large Polarization Effect Responsible for Excitonic Red Shifts in PbSe Quantum Dot Solids. *J. Phys. Chem. Lett.* **2011**, *2*, 795–800.

43 Deacon, G. B.; Phillips, R. J. Relationships Between the Carbon-Oxygen Stretching Frequencies of Carboxylato Complexes and the Type of Carboxylate Coordination. *Coord. Chem. Rev.* **1980**, *33*, 227–250.